International Journal of Engineering & Technology, 9 (2) (2020) 586-591

International Journal of Engineering & Technology

Website: www.sciencepubco.com/index.php/IJET

Research paper

A study for the prediction of corona power on electrostatic precipitator based on simple and easy two-dimensional electrostatic simulation

Chang-Hee Cho [1] *, Dong-Hoon Kim [2], Sang-Eon Park [3]

[1] Department of Precision Mechanical Engineering, Gyeonggi University of Science and Technology, Siheung, Korea
[2] Department of Mechanical Engineering, Graduate School, Inha University, Incheon, Korea
[3] Department of Business Administration, Graduate School, Sejong University, Seoul, Korea
**Corresponding author E-mail: choch@gtec.ac.kr*

Abstract

This study examines how the designing of an electrostatic precipitator can be carried out in a simple way. While it is of value to find out the theoretical values of design parameters using three-dimensional finite element model and numerical method, this study shows that employ-ing a two-dimensional finite element model and easily usable public-domain program is equally simple and fast. Variations of some physical properties occurring between an electrode and a duct are expressed using two design parameters. In this process, the design of the experi-ment and the response surface method are used based on the two-dimensional finite element model, as well as electrostatic simulation. A test using an electrostatic precipitator is performed and it is confirmed that a variation of corona power by the test is most similar with the varia-tion of stored energy by the simulation. A conversion factor that can predict corona power with the response surface function for the stored energy is proposed.

Keywords: *ESP; Electrostatic Simulation; Corona Power; RMS; DOE.*

1. Introduction

Over the last few decades, there have been ongoing researches on the global atmosphere and its related issues. Recently, there has been a growing interest in the treatment of particulate matter emitted from thermal power plants, incinerators, and manufacturing facilities [1]. Further, electrostatic precipitator (ESP) plays an essential role in removing gas or microparticles emitted from the industrial field [2]. ESP is the most efficient device used for the removal of fly ash particles from the flue gases produced by coal-fired boilers in power plants [3]. He et al. [4] developed the use of ESP instead of conventional filters to remove fine dust from air supplied to power plant gas turbines. ESP is now being used in a variety of fields due to its effectiveness in internal combustion engines, suppressing the re-entrainment phenomenon of the low-resistivity particles included in the gas emission [5], injection molding process [6], semiconductor manufacturing processes [7], ducted heat pump system [8], hospital wastes incineration [9], and collection of cement particle [10].

According to various applications, there are many studies about increasing the particle collection efficiency of ESP. Since energy consumption and CO2 emission can be increased by increasing dust collection capacity, Grass et al. [11] developed a control system that could increase dust collection efficiency while saving energy consumption. Takashima et al. [12] developed an ESP without corona discharge, using an induction charging-based particle charger and a parallel plate type particle collector, which reduced power consumption and restricted ozone production. Kim et al. [13] conducted an experiment to improve the collection efficiency of monodisperse nanometer-sized particles by combining ESP with an electrospray. Eshkevari et al. [14] carried out a research to reduce the size, weight, and cost of ESP while maintaining its efficiency by implementing a high-frequency power converter.

However, researches on the improvement of collection efficiency or design optimization, in most cases, were carried out by the use of complicated three-dimensional finite element model and numerical method. Yang et al. [15] analyzed gas-particle flow in the coupled electric field by the Eulerian-Lagrangian method in Computational Fluid Dynamics (CFD). Shen et al. [16] and Zheng et al. [17] investigated the effectiveness of electrodes by observing the electrohydrodynamic (EHD) flow surrounding the electrodes, using a computational fluid dynamics (CFD) code with the aid of a user defined function (UDF). Hamou et al. [18] used a complicated three-dimensional model and finite element method (FEM) to analyze the monopolar ionized field in the ESP. Porteiro et al. [19] proposed a complicated mathematical model to analyze particle flow near the electrode, while Guo et al. [20] proposed a CFD model based on the Eulerian-Lagrangian framework. The analysis of an electric field strength from the electrode till duct was likewise carried out with the development of the numerical model and through FEM [21].

The studies utilizing these three-dimensional finite element model and numerical method can guarantee their accuracy and the reliability of the results, but the research procedure is complicated and takes a long time. In addition, there are various unexpected variables in the

industry field. Even if the analysis is done systematically, there is a difference to some extent between the theoretical analysis results and actual phenomena. Therefore, it may be more efficient to predict actual test results in some cases based on the simulation results carried out with a simple and easy method, instead of consuming a long time in complicated research that excessively adheres to theoretical accuracy.

In this study, a method of roughly predicting the actual corona power of ESP with only electrostatic simulation for the simple two-dimensional finite element model is evaluated. Furthermore, the response surface function and conversion factor that can predict corona power according to design parameters are proposed in order to utilize the design of the electrode or duct in the future. For that, physical properties such as electric field, flux, and stored energy, which are generated between electrode and duct, were obtained from a two-dimensional electrostatic simulation. Moreover, the simulation results were compared with the corona power through an actual test for ESP. Response functions according to design parameters were obtained through the design of experiments (DOE) [22] and response surface method (RSM) [23]. A public domain code of FEMM 4.2 for electrostatic simulation was used for simple and easy study.

2. Two-dimensional electrostatic simulation and response surface function

2.1. Two-dimensional finite element model for electrostatic simulation

Figure 1 shows the illustration of the small-sized ESP prepared for the experiment, and the duct in the illustration is given a cross-section view to show the electrode inside. A cylindrical duct with an inner diameter of 108mm is used and it plays the role of electric ground. At the center of ESP, a row of electrodes is arranged, and the shape of each electrode resembles a star. The maximum width and thickness of the electrode are 28mm and 0.3mm, respectively. Both duct and electrode are made of stainless steel. The number of edges of the electrode illustrated in Figure 1 is 7.

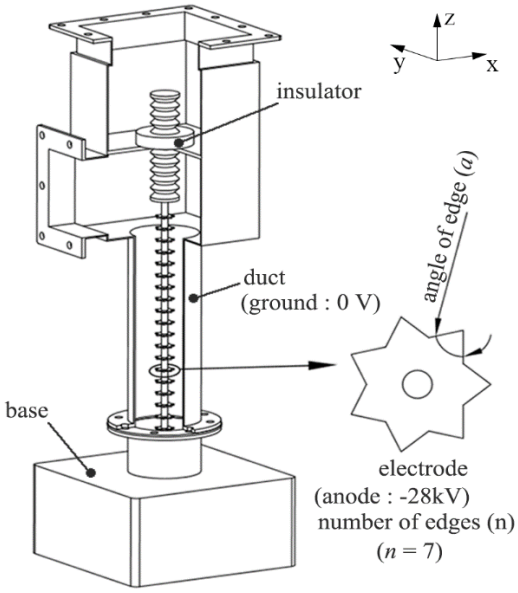

Fig. 1: Above Is the Layout of An ESP Test Model. This Duct Is A Cross-Section View That Shows the Electrodes. in This Study, the Design Parameters for the Electrode are the Angle of the Edge and the Number of Edges.

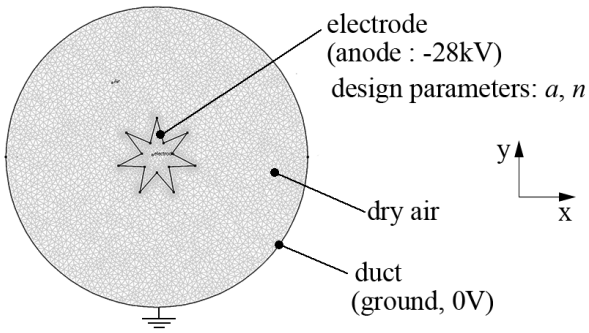

Fig. 2: Shown Is A Two-Dimensional Finite Element Model of Electrode and Duct for Electrostatic Simulation Where the Model Is A Cross-Sectional Cut of the Duct to the X-Y Plane in Figure 1.

Figure 2 shows a two-dimensional finite element model of the duct and electrode used for electrostatic simulation. This model is a cross-sectional cut of the duct to an x-y plane of Figure 1. At the center, there is an electrode that plays the role of an anode. The angle of edge of the electrode is 30º (a=30°), and the number of edges is 7 (n=7) as shown in Figure 2. The outer circle is the duct and is acting as a ground in the simulation. Dry air is filled between the electrode and duct. The depth of the finite element model is also set to 0.3mm as the thickness of the electrode is 0.3mm. Although it is different depending on the design parameters set of the finite element model, the number of nodes about the finite element model is 5,191 to 9,125, the number of the elements is 10,225 to 18,091, and the element type is a three-node triangular element.

2.2. Design of experiments and electrostatic simulation

Before designing a DOE, the major design parameters governing the corona power have to be identified. Although there is a considerable amount of design parameters affecting the corona power, the parameters are limited to the geometries of the duct and electrode, such as the shape and inner diameter of the duct, as well as the size, angle, and number of edges of the electrode. A rectangular shaped duct is practically installed for volume efficiency. However, since the rectangular part generates a non-asymmetric electric field, a circular duct is selected in this work. In addition, the inner diameter of the duct is related with the volume of the mass flow of the ESP, and it is not suitable as a parameter. A large size of electrode makes the distance between the electrode and duct closer. It is more helpful to generate a high level of corona power but it leads to instability due to air flow. Therefore, the angle of edge (a) and number of edges (n) are appropriate as design parameters in this work. For DOE, each parameter is chosen to have high and low level values as listed in Table 1.

Table1: Design Parameters Affecting the Electrostatic Simulation Result at Two Levels

Parameters	Low level	High level
Angle of edge, a (deg)	30	60
Number of edges, n	7	15

The electrostatic simulation results are summarized in Table 2 in terms of the physical properties for DOE. The DOE is built as a central composite design (CCD) [24] method enabling the expression of a 2nd order response surface function in order to determine the effect of curvature. The value of α is 1.414 since the number of design parameters is two, and the central point does not repeat because of the simulation test.

Table 2: Six Physical Property Values at Nine Points of the Central Composite Design for the Second-Order Response Model Whose Values are Obtained from Electrostatic Simulation

No.	a, deg	n	$\|E_{max}\|$, kV/mm	$\|D_{max.flux}\|$, C/mm^2	$\|F\|$, $\times10^{-11}$C	U_s, μJ	$\|D_{avg.flux}\|$, C/mm^2	$\|E\_avg\|$, μV/mm
1	30	7	20.37	180.3	3.24920	4.30486	1.90517	0.45505
2	60	7	15.68	138.9	3.28313	4.38122	4.94379	0.33965
3	30	15	18.58	164.5	1.60301	4.58065	2.36374	0.33531
4	60	15	15.28	135.3	1.64240	4.61706	1.87223	1.01618
5	45	11	17.64	156.2	2.19324	4.51269	1.56670	0.12513
6	23	11	21.41	189.5	2.17725	4.47919	1.08186	0.23019
7	67	11	11.26	99.68	2.17858	4.55138	3.35988	0.30103
8	45	5	18.54	164.2	4.77974	4.17092	0.99933	0.41735
9	45	17	16.85	149.2	4.37751	4.62596	3.72518	0.18063

In the actual test of ESP, the corona is generated and the electron moves from electrode to duct (current flows from duct to electrode) when the voltage of -28kV is supplied to the electrode. However, because the scope of this study is to introduce a simple research method to predict the actual corona power of ESP, the test of ESP is substituted to a two-dimensional electrostatic simulation. Meanwhile, the corona power is predicted using physical properties obtained from the simulation. The physical properties generated between electrode and duct in the two dimensional electrostatic simulation are as follows: magnitude of maximum electric field ($|E_{max}|$), magnitude of maximum density of flux ($|D_{max.flux}|$), quantity of flux ($|F|$), stored energy in the volume (U_s), magnitude of average density of flux in the volume ($|D_{avg.flux}|$), and magnitude of average electric field in the volume ($|E\_avg|$). Among the physical properties, one of the most similar with corona power is selected by the comparison analysis.

2.3. Response surface function for each physical value

The second-order response surface function for each physical property can be derived by analyzing values in Table 2. Response surface function is expressed as first and square terms for two variables, and it can provide enhanced optimization. From Table 2 and RSM, response surface function for the magnitude of maximum electric field ($|E_{max}|$) can be expressed as:

$$|E_{max}|=25.309-0.0117a-0.4783n-0.0019a^2+0.0152n^2 \text{ (kV/mm)} \quad (1)$$

Here, it is assumed that interaction between parameters is ignored through analysis about their main effects. Since the coefficient of determination (R^2 = 1-Residual sum of square/Total sum of square) for (1) is 0.924, (1) is accurate within the 8% error [25].
Also there is no interaction between two parameters for the magnitude of maximum density of flux ($|D_{max.flux}|$), quantity of flux ($|F|$), and stored energy in the volume (U_s) from Table 2 and, thus, the response surface function for each property is expressed as follows:

$$|D_{max.flux}|=225.86-0.146a-4.435n-0.017a^2+0.144n^2 \text{ (C/mm}^2\text{)} \quad (2)$$

$$|F|=5.17502+0.19045a-1.11844n-0.00211a^2+0.04536n^2 \text{ (}\times10^{-11}\text{C)} \quad (3)$$

$$U_s=3.7243-0.00155a+0.10496n+0.00004a^2-0.00313n^2 \text{ (μJ)} \quad (4)$$

The coefficients of determination for (2), (3), and (4) are 0.924, 0.914, and 0.987, respectively, in which the average is close to 1.0.
Meanwhile, there is an interaction between two parameters for the magnitude of average density of flux in the volume ($|D_{avg.flux}|$) and magnitude of average electric field in the volume ($|E_{avg}|$) from Table 2. The interaction term is added to the response function and is expressed as:

$$|D_{avg.flux}|=1.38001-0.0169a-0.17601n+0.00252a^2+0.03985n^2-0.01471a\cdot n \text{ (fC/mm}^2\text{)} \quad (5)$$

$$|E_{avg}|=4.70943-0.10989a-0.43669n+0.00088a^2+0.01338n^2+0.00332a\cdot n \text{ (μV/mm)} \quad (6)$$

In these equations, the coefficients of determination for (5) and (6) are 0.624 and 0.770, respectively.

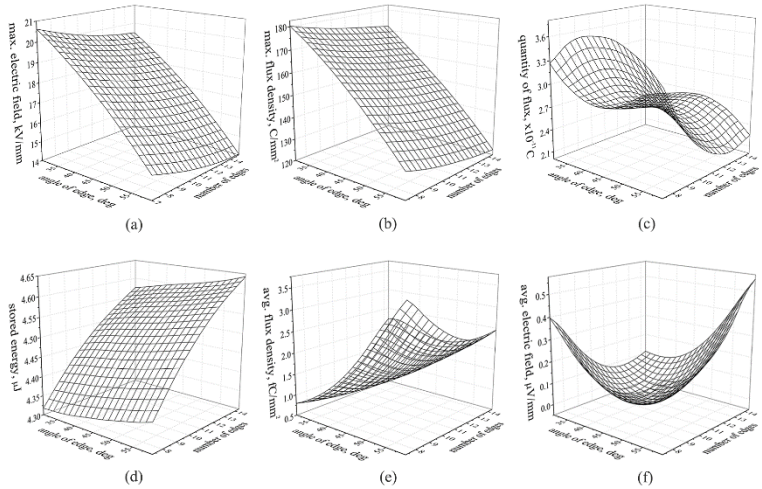

Fig. 3: This Is the Surface Wire Frame Plot of Response Functions with Respect to the Angle of Edge and the Number of Edges: (A) Magnitude of Maximum Electric Field ($|E_{max}|$), (B) Magnitude of Maximum Density of Flux ($|D_{max.Flux}|$), (C) Quantity of Flux ($|F|$), (D) Stored Energy in the Volume (U_s), (E) Magnitude of Average Density of Flux in the Volume ($|D_{avg.Flux}|$), and (F) Magnitude of Average Electric Field in the Volume ($|E_{avg}|$). in the Study, the Inner Diameter of Duct Is 108mm, and the Size, Thickness, and Inlet Voltage of Electrode are 28mm, 0.3mm, and -28kv, Respectively.

Figure 3 shows the surface wire frames plot for six physical properties using (1) - (6). For Figure 3(a) and Figure 3(b), the parameter of angle of edge (a) gives a higher main effect than the number of edges (n) about magnitude of maximum electric field and magnitude of maximum density of flux, whereas the shape of the two surfaces are similar except for the values. The location where generate flux and electric field by maximum value is the same as end of the electrode is shown in Figure 2. Thus, for the micro-element, the magnitude of maximum density of flux can be similar with magnitude of maximum electric field, which is integrated into flux. As shown in Figure 3(c), the amount of flux generated over an entire finite element model shows greatly changed curvature. In addition, a low value of the number of edges leads to further generation of flux. The stored energy for the entire finite element is also varied to a slope with moderate curvature, as in Figure 3(d), which signifies that more energy can be stored when the electrode has more edges. Figure 3 (e) and Figure 3 (f) show stationary points within two levels of design parameters, allowing the optimization of the design parameters immediately. However, the coefficients of determination (5-6) are lower than 0.8, and the reliability of response surface is suspicious.

3. Tests with ESP and comparison of electrostatic simulation

3.1. Tests with ESP

For the test with ESP, where voltage is supplied to the electrode, corona power (P_c) can be measured. The tests are performed according to the DOE of Table 2 and then the response surface function for corona power by two parameters (angle of edge and number of edge) can be obtained. From comparison with the response surface plot for corona power and Figure 3, the most similar variation of physical property with variation of corona power can be found. Figure 4 shows the equipment for a test with ESP, and the geometry of the equipment, including the electrode, is approximately similar with the layout in Figure 1. However, since the testing equipment is a three-dimension model, 16 electrodes are arranged at one row with a 26mm pitch. The test is carried out by supplying a voltage to the electrode and measuring the corona current generated between the electrode and duct. Furthermore, corona power can be derived from voltage and current (power = voltage × current).

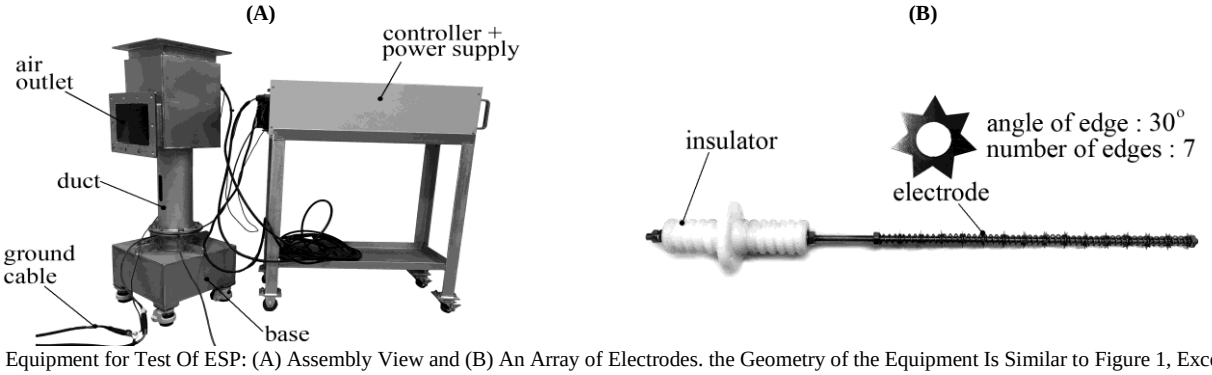

Fig. 4: Equipment for Test Of ESP: (A) Assembly View and (B) An Array of Electrodes. the Geometry of the Equipment Is Similar to Figure 1, Except for An Array of Electrodes.

Table 3: Below Are the Corona Power Values at the Nine Points of the Central Composite Design for the Second-Order Response Model. the Values of Corona Power are Obtained from the Test.

No.	a, deg	N	P_c, W
1	30	7	2.816
2	60	7	3.211
3	30	15	3.111
4	60	15	3.611
5	45	11	3.354
6	23	11	3.388
7	67	11	3.521

8	45	5	2.699
9	45	17	3.789

In the DOE for the test, selected values of high level and low level for the two parameters and combination are the same as Table 1 and Table 2. The test results are summarized in Table 3 in terms of corona power for DOE. The response surface function about corona power (P_c) obtained from Table 3 and RSM can be expressed as:

$$P_s=0.9558+0.0213a+0.2568n-0.000136a^2-0.008496n^2 \text{ (W)} \quad (7)$$

In this equation, interaction is ignored from the determination about the main effects for two parameters. The coefficient of determination (7) is 0.850, which is close to 1.0 and it is appropriate.
Figure 5 shows the surface wire frame plot of the corona power according to two design parameters (7). The plot forms a slope with a small curvature. The higher values of both design parameters lead to the generation of more corona power, with the main effect for the parameter of the number of edges being higher than the main effect for the angle of edge. Since the stationary point cannot be found in Figure 5, the optimization values for each design parameter are out of the table.

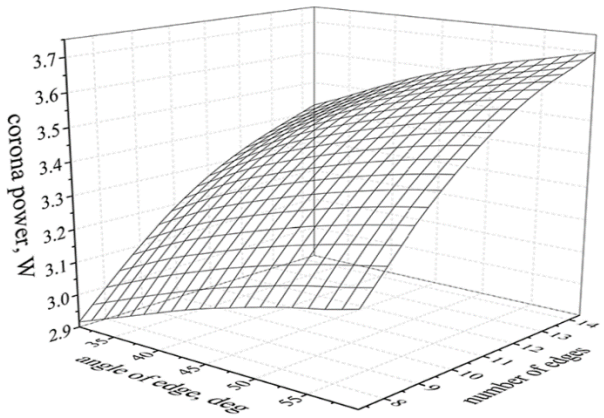

Fig. 5: Above Is the Surface Wire Frame Plot of Corona Power with Respect to the Angle of Edge and the Number of Edges. Conditions and Design Parameters of the Test Are Similar with Electrostatic Simulation Except for One in Which One Array of 16 Electrodes are Used in the Test.

3.2. Conversion factor for the prediction of corona power using electrostatic simulation

Comparison between test results in Figure 5 and simulation results in Figure 3 reveal that variation of stored energy (U_s) according to two design parameters, among the six physical properties, is most similar with the variation of corona power (P_c) under the same condition. The directions of two design parameters affecting the object function are equal and both have moderate curvature in the surface plot. However, the values of the main effects for the two parameters are different while the corona power shows more deviation in the main effect for the two design parameters.
A simple and easy method to predict test results from the simulation is to use the conversion factor. Because of the second order response surface function, a conversion factor is multiplied for each coefficient in each term of the response surface function obtained from the simulation (4); thus, the coefficient of response surface function from the test (7) can be equal. Therefore, the predicted corona power (P_{prd}) derived from the stored energy can be expressed as a combination (4), and the conversion factor is as follows:

$$P_{prd}= C_0\cdot3.7243-C_1\cdot0.00155a+C_2\cdot0.10496n+C_3\cdot0.00004a^2-C_4\cdot0.00313n^2 \text{ (W)} \quad (8)$$

The conversion factor can be found out to make it equivalent to (8) and (7):

$$C_0=0.257,\ C_1=-13.742,\ C_2=2.447,\ C_3=-3.4,\ C_4=2.714 \quad (9)$$

The coefficient of determination (R^2) means regression ratio of the equation from tests. The coefficient of determination for (4) (value is 0.978) and (7) (value is 0.850) can be inferred as regression ratio from numerical test and actual test, respectively. Thus, the predicted corona power of (8) with conversion factor of (9) can express actual test within 16.9% error.
From two simple dimensional electrostatic simulations, the second order response surface function for the stored energy such as (4) can be expressed. Subsequently, the conversion factor (9) applies to the response surface function, and the response surface function for predicted corona power (P_{prd}) can be derived with the test. With the same method, the value of corona power can be predicted without the test even though the two parameters of angle of edge and number of edges are changed. Additionally, the conversion factor will be useful for achieving the optimization of the design parameters in the future.

4. Conclusion

A conversion factor to predict the test results of ESP by using the simulation results of the simple two- dimensional electrostatic simulation was proposed. Without numerical analysis with three-dimensional finite model or test, the corona power was derived simple and easily. In addition, the corona power of ESP could be substituted to stored energy under two-dimensional electrostatic simulations. The function of the predicted corona power and conversion factor will be useful for the design of the electrode and duct of the ESP, and the simple way this can work can be applied in the study about design optimization in various fields.
However, this study did not consider the effect by the arrangement of electrodes in the three-dimensional ESP. In the tests, corona power was affected by the quantity and pitch of the electrode, but such parameters could not be considered in the two-dimensional electrostatic simulation. Therefore, the effect of the parameters should be expressed as another conversion factor. Moreover, the conversion factor will

be suitable only in ESP with similar geometry of this study. This study will be useful to show a process which predict actual test result from simple numerical test result, but utilization of the conversion factor will be limited. This problem needs to be addressed in the future.

Acknowledgement

This work was supported by the Korea Institute of Energy Technology Evaluation and Planning (KETEP) and the Ministry of Trade, Industry & Energy (MOTIE) of the Republic of Korea (No. 20171120100530)

References

[1] Li S, Huang Y, Zheng Q, Deng G & Yan K, "A numerical model for predicting collection efficiency of electrostatic precipitator", *Power Technology*, Vol.347, (2019), pp.170-178. https://doi.org/10.1016/j.powtec.2019.02.040.

[2] Jaworek A, Sobczyk AT, Marchewicz A, Krupa A, Czech T, Ottawa A &Charchalis A, "Two-stage vs. two-field electrostatic precipitator", *Journal of Electrostatics*, Vol.90, (2017), pp.106-112. https://doi.org/10.1016/j.elstat.2017.10.006.

[3] Jaworek A, Marchewicz A, Sobczyk AT, Krupa A & Czech T, "Two-stage electrostatic precipitators for the reduction of PM2.5 particle emission", *Progress in Energy and Combustion Science*, Vol.67, (2018), pp.206-233. https://doi.org/10.1016/j.pecs.2018.03.003.

[4] He Z, Dass ETM & Karthik G, "Design of electrostatic precipitator to remove suspended micro particulate matter from gas turbine inlet airflow: Part I. Experimental study", *Journal of Aerosol Science*, Vol.108, (2017), pp.14-28. https://doi.org/10.1016/j.jaerosci.2017.03.003.

[5] Yamamoto T, Maeda S, Ehara Y & Kawakami H, "Development of EHD-assisted plasma electrostatic precipitator", *IEEE Transactions on Industry Applications*, Vol.49(2), (2013), pp.672-678. https://doi.org/10.1109/TIA.2013.2241378.

[6] Son C, Lee W, Jung D, Lee D, Byon C & Kim W, "Use of an electrostatic precipitator with wet-porous electrode array for remove of air pollution at precision manufacturing facility", *Journal of Aerosol Science*, Vol.100, (2016), pp.118-128. https://doi.org/10.1016/j.jaerosci.2016.07.005.

[7] Chen TM, Tsai CJ, Yan SY & Li SN, "An efficient wet electrostatic precipitator for removing nanoparticles, submicron and micron-sized particles", *Separation and Purification Technology*, Vol.136, (2014), pp.27-35. https://doi.org/10.1016/j.seppur.2014.08.032.

[8] Song CH, Woo CG, Han B, Kim HJ, Kim YJ, Kim OJ & Yoon SH, "Parametric study of wet electrostatic precipitator applied to ducted heat pump system", *International Journal of Air-conditioning and Refrigeration*, Vol.26, No.2, (2018), pp.1850019.1-1850019.7 https://doi.org/10.1142/S2010132518500190.

[9] Miloua F, Tilmatine A, Remaoun SM, Bengrit M, Zouzou N & Dascalescu L, "Development of a cost-efficient electrostatic precipitator for hospital wastes incineration", *IEEE, Industry Applications Society Annual Meeting*, Oct., (2013), pp.1-5. https://doi.org/10.1109/IAS.2013.6682464.

[10] Kherbouche F, Benmimoun Y, Tilmatine A, Zouaghi A & Zouzou N, "Study of a new precipitator with asymmetrical wire-to-cylinder configuration for cement particles collection", *Journal of Electrostatics*, Vol.83, (2016), pp.7-15. https://doi.org/10.1016/j.elstat.2016.07.001.

[11] Grass N, Zintl A & Hoffmann E, "Electrostatic precipitator control system", *IEEE Industry Applications Magazine*, Vol.16, No.4, (2010), pp.28-33. https://doi.org/10.1109/MIAS.2010.936967.

[12] Takashima K, Kohno H, Katatani A, Kurita H & Mizuno A, "Two-stage electrostatic precipitator using induction charging", *Journal of Physics: D. Applied Physics*, Vol.51, No.17, (2018), pp.174002. https://doi.org/10.1088/1361-6463/aab4bf.

[13] Kim JH, Lee HS, Kim HH & Ogata A, "Electrospray with electrostatic precipitator enhances fine particles collection efficiency", *Journal of Electrostatics*, Vol.68, No.4, (2010), pp.305-310. https://doi.org/10.1016/j.elstat.2010.03.002.

[14] Eshkevari AL, Farzi M & Arefian M, "Design of a new high-frequency power converter for electrostatic precipitators", *Power Electronics, Drives Systems and Technologies Conference 2018 9th Annual*, (2018), pp.289-293. https://doi.org/10.1109/PEDSTC.2018.8343811.

[15] Yang D, Guo B, Ye X, Yu A & Guo J, "Numerical simulation of electrostatic precipitator considering the dust particles space charge", *Powder Technology*, Vol.354, (2019), pp.552-560. https://doi.org/10.1016/j.powtec.2019.06.013.

[16] Shen H, Yu W, Jia H & Kang Y, "Electrohydrodynamic flows in electrostatic precipitator of five shaped collecting electrodes", *Journal of Electrostatics*, Vol.95, (2018), pp.61-70. https://doi.org/10.1016/j.elstat.2018.08.002.

[17] Zheng C, Zhang X, Yang Z, Liang C, Guo Y, Wang Y & Gao X, "Numerical simulation of corona discharge and particle transport with the particle space charge effect", *Journal of Aerosol Science*, Vol.118, (2018), pp. 22-33. https://doi.org/10.1016/j.jaerosci.2018.01.008.

[18] Hamou N, Massinissa A, Hakim A & Youcef Z, "Finite element method investigation of electrostatic precipitator performance", *International Journal of Numerical Modeling: Electronic Network, Devices and Fields*, Vol. 28, No. 2, (2018), pp.138-154. https://doi.org/10.1002/jnm.1992.

[19] Porteiro J, Martin R, Granada E & Patino D, "Three-dimensional model of electrostatic precipitator for the estimation of their particle collection efficiency", *Fuel Processing Technology*, Vol.143, (2016), pp.86-99. https://doi.org/10.1016/j.fuproc.2015.11.010.

[20] Guo B, Yu A & Guo J, "Numerical modeling of ESP for design optimization", *Procedia Engineering*, Vol.102, (2015), pp.1366-1372. https://doi.org/10.1016/j.proeng.2015.01.268.

[21] Popa GN, Dinis CM & Deaconu SI, "Numerical modelling in plate-type electrostatic precipitator supplied with pulse energization" *Power Electronics and Applications, Proceedings of the 2011-14th European Conference*, (2011), pp.1-8.

[22] Taguchi G, *System of experimental design: engineering methods to optimize quality and minimize cost*, White Plains, NY, UNIPUB/Kraus International, (1987).

[23] Myers RH, Montgomery DC & Anderson-cook CM, *Response surface methodology: process and product optimization using designed experiment 3/e*, New Jersey, Wiley-Interscience Publication, (2009).

[24] Khuri AI & Cornell JA, *Response surface: design and analysis 2/e*, NY, Marcel Dekker, (2005).

[25] Cho CH, Kim YG, Chae SW & Kim KH, "Design of a LCD display stand for maximum turnover safety," *Journal of Mechanical Science and Technology*, Vol. 30, No. 4, (2016), pp.1705-1712. https://doi.org/10.1007/s12206-016-0326-z.